WOOD RESEARCH
57 (4): 2012
669-676

SHORT NOTE

MECHANICAL PROPERTIES AND FAILURE BEHAVIOUR OF YEW AND SPRUCE DETERMITED WITH A COMPACT TENSION TEST AND DIGITAL IMAGE CORRELATION

Daniel Keunecke, Peter Niemz
Eth Zürich, Institute for Buildings Materials, Wood Physics
Zürich, Switzerland

Markus Tollert, Andreas Hänsel
Berufsakademie Sachsen, Staatliche Studienakademie Dresden
Dresden, Germany

(Received January 2011)

ABSTRACT

While the longitudinal mechanical behaviour of Common yew is relatively well known, only limited information is available about its behaviour when the load direction is oriented perpendicular to the grain. Thus in this study, a compact tension test was performed on small yew specimens (and on spruce as a reference species) for four different crack orientations. The experiment was supplemented by a digital image correlation system to analyse the strain in fracture process zones on the surface of the samples. Various relevant mechanical parameters (critical load, initial stiffness and fracture toughness) were determined and evaluated. Better mechanical properties were obtained for yew as a result of its higher raw density compared with spruce. Several further characteristics were interpreted against the background of structure-property relationships.

KEYWORDS: Compact tension test, digital image correlation, fracture toughness, fracture process zone, common yew, Norway spruce.

INTRODUCTION

From a technological point of view, the softwood species Common yew (*Taxus baccata* L.) is regarded as highly deformable in the longitudinal direction and is able to absorb a large amount of energy during deformation. Most of the few available literature references report elastic moduli between 6.2 and 12 GPa for yew (e.g. Sekhar and Sharma 1959, Jakubczyk 1966, Wagenführ 2000, Märki et al. 2005), which is low with respect to its relatively high raw density (about

650 kg.m^{-3} or even higher) and can be ascribed to high microfibril angles, and maybe also to the relatively small density gradient between earlywood (EW) and latewood (LW). Thus yew holds a distinctive position among softwoods regarding its longitudinal deformability and is predestined for case studies with regard to structure-function relationships.

However, clearly less is known about its elastic and fracture-mechanical behaviour when the load direction is oriented perpendicular to the grain. Thus the goal of this study was to investigate these load cases for yew wood (and for spruce as a reference species) and to determine certain relevant mechanical properties and the influence of parameters such as the crack tip position. We decided to carry out compact tension (CT) tests as a continuation of previous studies performed against a similar background (Märki et al. 2005, Keunecke et al. 2007). With CT tests, relatively stable crack propagation can be achieved and small specimens can be evaluated. The latter is crucial in the case of yew, since its wood is characterised by many irregularities: The growth ring boundaries are often wavy, and a larger quantity of encased dead knots and irregular grain complicates the production of clear specimens as do large amounts of compression wood.

MATERIAL AND METHODS

The CT test was performed on spruce (*Picea abies* (L.) Karst.) and yew (*Taxus baccata* L.) specimens (Fig. 1a), each taken from one board per tree. The starter notch was additionally sharpened with a razor blade. Raw density was determined gravimetrically after the specimens reached equilibrium moisture content (spruce: about 12 %, yew: about 11 %) during storage at 20°C and 60 % relative air humidity.

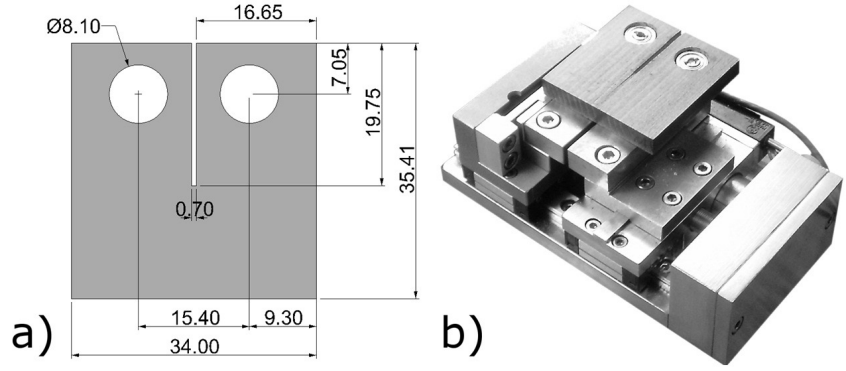

Fig. 1: a) Geometry of the CT specimens with all dimensions in (mm); the thickness was 5 mm, b) Universal micro stage with a specimen readily prepared for a CT experiment.

The CT experiment was performed using an MT300 universal micro stage (Deben, UK) for small specimens (Fig. 1b). The maximum load capacity was 300 N, and the feed-rate was displacement-controlled by the Software Microtest 5.5.19. It was chosen such that the maximum load was reached in 90 (±30) s. The tests were carried out in the RL, TL, RT and TR orientations (the first letter indicates the load direction; the second gives the direction of crack propagation; L, R, T represent the principal directions longitudinal, radial, tangential). About 11 specimens

per crack orientation (the exact number can be seen in Tab. 1) were tested.

Tab. 1: Characteristic results of the compact tension test.

	Crack orientation	Crack tip position	n		ρ (kg.m^{-3})	ω (%)	k_{init} (N.mm^{-1})	F_{crit} (N)	K_{IC} (MPa√m)
Spruce	RL	EW	7	$\bar{x}$	474	12.5	78.6	27.5	0.22
				CoV (%)	1.28	2.21	10.1	10.6	10.99
		LW	4	$\bar{x}$	472	12.6	80.8	31.3	0.25
				CoV (%)	0.80	3.38	2.12	8.88	8.85
	TL	-	11	$\bar{x}$	440	12.8	66.8	23.8	0.19
				CoV (%)	4.06	5.55	9.21	13.0	12.1
	RT	EW	6	$\bar{x}$	472	12.3	20.3	20.2	0.16
				CoV (%)	0.78	3.32	6.35	3.20	3.10
		LW	5	$\bar{x}$	473	12.0	20.9	21.2	0.17
				CoV (%)	1.23	3.63	2.01	8.69	8.98
	TR	EW	6	$\bar{x}$	453	12.3	17.2	18.0	0.16
				CoV (%)	0.65	3.33	2.14	17.8	1.05
		LW	5	$\bar{x}$	456	12.8	18.1	19.6	0.14
				CoV (%)	0.49	13.9	3.88	1.02	18.2
Yew	RL	EW	12	$\bar{x}$	527	11.0	112.9	38.6	0.30
				CoV [%]	1.29	4.97	9.35	5.50	5.50
		LW	-	$\bar{x}$	-	-	-	-	-
				CoV [%]	-	-	-	-	-
	TL	-	7	$\bar{x}$	506	11.2	68.1	26.6	0.21
				CoV [%]	3.51	4.07	10.7	8.99	8.64
	RT	EW	10	$\bar{x}$	600	10.5	56.2	27.2	0.22
				CoV [%]	2.43	3.36	11.1	9.64	9.75
		LW	1	$\bar{x}$	600	10.3	55.9	30.32	0.24
				CoV [%]	-	-	-	-	-
	TR	EW	6	$\bar{x}$	577	11.0	53.9	25.7	0.20
				CoV [%]	2.51	3.18	8.85	10.7	10.8
		LW	5	$\bar{x}$	566	10.9	52.1	23.6	0.19
				CoV [%]	2.24	3.66	8.30	6.69	6.99

RL radial-longitudinal, TL tangential-longitudinal, RT radial-tangential, TR tangential-radial, n number of specimens, EW earlywood, LW latewood, x mean value, CoV coefficient of variation, ρ air-dry density, ω equilibrium moisture content at 20°C and 65 % relative humidity, k_{init} initial slope of the load-displacement graph, F_{crit} critical load (end of the linear-elastic phase in the load-displacement diagram), K_{IC} critical stress intensity value.

To evaluate the surface displacements of the specimens, a high-contrast speckle pattern was sprayed on the top surfaces using an airbrush gun and finely pigmented acrylic paint. Such patterns were necessary for evaluation with digital image correlation (DIC) (for further details, see Keunecke et al. (2008)). The used DIC software was VIC 3D (Correlated Solutions), a video image correlation system. It allows full-field surface tracking of the sample deformations

and computing strain distribution based on grey value cross-correlations of the speckle pattern recorded via two CCD cameras. Its correlation algorithm is based on the principle of the allocation of equal grey value patterns and therefore is able to track the displacement of small neighbourhoods. During the CT test, the specimen surfaces were filmed with a resolution of about 1400 x 1400 pixels at a capture frequency of 5 Hz.

Three material characteristics were determined:

- the critical load F_{crit} representing the end of the linear elastic phase and thus indicating macrocrack initiation (Frühmann et al. 2003),
- the initial stiffness k_{init} representing the linear-elastic phase of the load-displacement diagram (a parameter proportional to the effective modulus of elasticity; Harmuth et al. 1996),
- the fracture toughness K_{IC}, a parameter characterising the ability of a material to withstand flaws that initiate failure. This was determined according to the following equation:

$$K_{IC} = \frac{F_Q}{B \cdot \sqrt{W}} \cdot f(a/W) \quad \text{(MPa m 0.5)} \tag{1}$$

where: K_{IC} - the fracture toughness,
F_Q - the critical force,
a - the crack length at the beginning of the test,
B - the specimen thickness,
W - the specimen width,
$f(a/W)$ - a geometry equation (for a/W = 0.50 applies: = 9.66):

$$f(a/W) = (2 + a/W) \cdot \frac{0.886 + 4.64(a/W) - 13.32(a/W)^2 + 14.72(a/W)^3 - 5.6(a/W)^4}{(1 - a/W)^{1.5}} \tag{2}$$

RESULTS AND DISCUSSION

A crucial precondition for the application of LEFM is that the fracture process zone (FPZ) is completely covered by the specimen. This was the case in our study as can be seen in Fig. 2 showing the horizontal strain of the samples during maximum load. The FPZ in yew was small, concentrated and oval (Fig. 2e-h), while the spruce FPZ was generally larger and of circular shape (Fig. 2a-d). The higher strains of yew directly in front of the crack tip indicate a high local elasticity.

In all crack orientations, yew reached higher maximum loads, K_{IC} values and stiffnesses (k_{init}) than spruce (Tab. 1). This can be ascribed to the 20 to 25 percent higher air-dry density of the yew samples; the vital influence of the density on mechanical properties when wood is loaded perpendicular to the grain is well known. The reinforcing effect of wood rays is reflected in the established principle that mechanical properties are better / higher in the RL than in the RT orientation, and better / higher in the RT than in the TR orientation, which was fully confirmed by our results. The most conspicuous differences between both species were found for k_{init} in the TR and RT crack orientation, where yew achieved almost three times higher values than spruce.

The fact that the overall K_{IC} values were up to 50 percent lower than those stated by Märki et al. (2005) for larger specimens must be ascribed to a size effect.

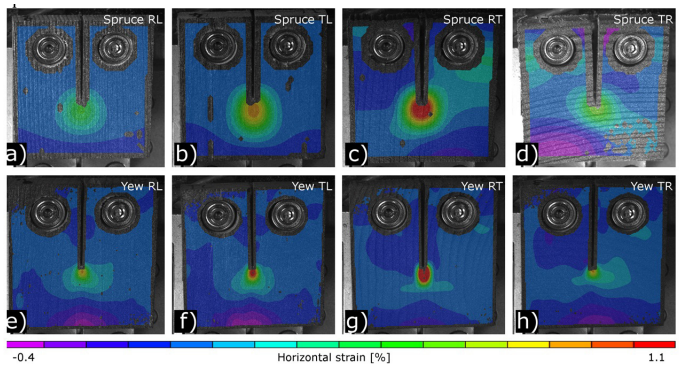

Fig. 2: Horizontal strain on the surface of CT specimens when the load maximum is reached. The figure shows representative spruce a)-d) and yew e)-h) specimens of the four crack orientations.

Märki et al. reported K_{IC} values of 0.56 KJ.m^{-2} (RL) and 0.46 KJ.m^{-2} (TL) for yew and 0.37 KJ.m^{-2} (RL) and 0.23 KJ.m^{-2} (TL) for spruce.

In the diagrams of Fig. 3, "displacement" is a parameter proportional to the crack mouth opening displacement of the specimens and was recorded by the linear variable differential transformer (LVDT) of the micro stage. The curves determined with an RL experiment show similar characteristics for both wood species: after reaching the maximum load, a sudden large drop in load accompanies the macro failure (crack propagation in the EW tissue). In the TL

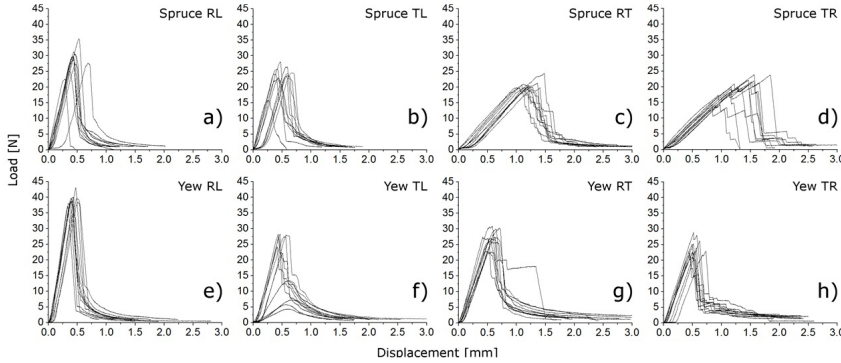

Fig. 3: Load-displacement diagrams of spruce a)-d) and yew e)-h) test series. "Displacement" represents the horizontal displacement of the loading head.

orientation, the curves look similar for spruce, while the yew curves are typically characterised by a step-wise load-drop after passing the maximum load. It is open to speculation whether the differences between both species are due to the fact that their LW tissues have similar densities while the EW density of yew is clearly higher than that of spruce. Incidentally, the three yew curves with the lowest load maximum are shown here but were not considered in the calculation of the values in Tab. 1 since they featured a certain pre-damage and were thus useless.

In the RT direction, the highest stability of crack propagation, characterised by short-term

phases of arrest before crack propagation, was observed. For yew, the propagation was even more stable than for spruce. This can be due to the rounder cross-sectional shape of yew tracheids compared to spruce, accompanied by less contact area between two adjacent tracheids. In the TR orientation, two failure patterns can be observed: some specimens showed a stepwise load drop with the crack tip arresting in the transition zone between EW and LW tissue, before a sufficient high load increase enabled the crack to pass the next LW zone. Other specimens showed a larger sudden load drop while the crack propagated across more than one growth-ring boundary, followed again by smaller stepwise load drops.

In most of the CT experiments, we observed the fibre bridging phenomenon. This is a process where - during crack propagation - single tracheids or tracheid bundles bridge the gap between both fracture surfaces and thus create an additional connection between them. This fracture-toughening mechanism was described by Vasic and Smith (2002), amongst others, and plays a major role in dissipation of fracture energy. For all orientations it can be generally stated that fibre bridging in spruce was accomplished by individual tracheids, while in yew whole tracheid bundles were also involved. In the RL orientation, fibre bridging was only occasionally found (more frequently in yew than in spruce). In the RL direction, almost no fibre bridging was observed for spruce, while it appeared frequently for yew. In the RT direction, fibre bridging occurred frequently for both species. But while it was found across the whole growth ring for yew, it was only visible in the LW zones of spruce. In the RT direction, it was observed for both species as well. Altogether, the overriding impression is that fibre bridging strongly depends on density (the higher the density, the higher the probability of fibre bridging), and the mechanical properties generally depend on the position of the initial crack tip. The latter can be viewed in Tab. 1, where the EW and LW parameters are listed separately.

CONCLUSIONS

Data evaluation revealed differences between yew and spruce samples that can be ascribed to their specific structure-property relationships. The high density of yew, for instance, obviously abets the occurrence of fibre bridging, and the initial crack tip position in pre-notched specimens is crucial for the identified mechanical properties (as Tab. 1 indicates) since the initial FPZ develops around this tip. The deviation from results of a similar experiment performed on larger specimens can be ascribed to a size effect. Future experiments should aim for deeper analysis of the FPZ with the inclusion of in-situ observation of material behaviour. This can result in additional information about the failure processes, especially at the micro level. The challenge, however, will be to find a practicable way to combine the diverse available experimental techniques (testing stages, DIC, microscopy).

In general, however, the CT tests have shown that the miniature CT test in combination with DIC is suitable for analysing mechanical parameters, the development of the FPZ and failure characteristics of wood samples. However, it would be advantageous to use another type of testing stage (servo-hydraulically driven) that is able to quickly respond to load drops. In doing so, the aim should be to achieve really stable crack propagation. This would entail the ability to determine further relevant fracture-mechanical parameters such as fracture energy. Another drawback is that data evaluation is still fairly laborious and time-consuming. However, this problem will be eliminated/significantly reduced in future studies, as one will be able to revert to more powerful computers requiring less calculation time.

REFERENCES

1. Frühmann, K., Burgert, I., Stanzl-Tschegg, S., Tschegg, E., 2003: Mode I fracture behaviour on the growth ring scale and cellular level of spruce (*Picea abies* (L.) Karst.) and beech (*Fagus sylvatica* L.) loaded in the TR crack propagation system. Holzforschung 57(6): 653-660.
2. Harmuth, H., Rieder, K., Krobath, M., Tschegg, E., 1996: Investigation of the nonlinear fracture behaviour of ordinary ceramic refractory materials. Mater. Sci. Eng. A Struct. Mater. 214(1): 53–61.
3. Jakubczyk, B., 1966: Technical properties of the yew wood from the preserve Wierzchlas. (Techniczne własności drewna cisa z rezerwatu Wierzchlas). Sylwan 110(10): 79-86 (in Polish).
4. Keunecke, D., Stanzl-Tschegg, S., Niemz, P., 2007: Fracture characterisation of yew (*Taxus baccata* L.) and spruce (*Picea abies* (L.) Karst.) in the radial-tangential and tangential-radial crack propagation system by a micro wedge splitting test. Holzforschung 61(5): 582-588.
5. Keunecke, D., Hering, S., Niemz, P., 2008: Three-dimensional elastic behaviour of common yew and Norway spruce. Wood Sci. Technol. 42(8): 633-647.
6. Märki, C., Niemz, P., Mannes, D., 2005: Vergleichende Untersuchungen zu ausgewählten mechanischen Eigenschaften von Eibe und Fichte. Schweiz. Z. Forstwes. 156(3/4): 85-91.
7. Sekhar, A.C., Sharma, R.S., 1959: A note on mechanical properties of *Taxus baccata*. Indian Forester 85: 324-326.
8. Vasic, S., Smith, I., 2002: Bridging crack model for fracture of spruce. Eng. Fract. Mech. 69(6): 745–760.
9. Wagenführ, R., 2000: Holzatlas. 5. Auflage, Fachbuchverlag Leipzig, München, 707 pp.

Daniel Keunecke, Peter Niemz
Eth Zurich
Institute for Buildings Materials, Wood Physics
Schafmattstrasse 6
8093 Zurich
Switzerland
Phone: +41 – 44 – 632 32 30
Corresponding author: niemzp@ethz.ch

Markus Tollert, Andreas Hänsel
Berufsakademie Sachsen
Staatliche Studienakademie Dresden
Heideparkstrasse 8
01099 Dresden
Germany